

THE STUDY OF α – *PARTICLE* INDUCED REACTION
ON GALLIUM ISOTOPES

A thesis submitted to the School of Graduate Studies
Addis Ababa University



In partial Fulfilment of the Requirements for the
Degree of Master of Science in Physics

By

Awoke Taddesse

Addis Ababa, Ethiopia

July 2007

ADDIS ABABA UNIVERSITY
FACULTY OF SCIENCE
DEPARTMENT OF PHYSICS

The undersigned hereby certify that they have read and recommended to the Faculty of Science School of Graduate Studies for acceptance a thesis entitled “**The study of α – particle induced reaction on gallium isotopes**” by in partial fulfillment of the requirements for the degree of **Master of Science in Physics**.

Name	Signature
Prof. Dr. A.K Chabey, Advisor	-----
Dr.Tilahun Tesfaye, Examiner	-----
Prof. Dr. Singh K.P, Examiner	-----

Dedicated

to

my wife and children.

Acknowledgements

I would like to thank Professor Dr. A.K Chaubey, my supervisor, for his many suggestions and constant support during this thesis. I am also thankful to physics department for supplying computers in our nuclear physics lab., without which this work would have been difficult to be completed. Finally I would like to give my great thanks to my friends especially to Talefe Eshete, Fikadu Nire and Abera Debebe for their constant support and encouragement. skills.

Addis Ababa, Ethiopia

Awoke Taddesse

Abstract

Alpha particle induced reaction on the two gallium isotopes has been studied in the intermediate energies up to 70MeV. The excitation functions of the six reaction channels were calculated using the semi classical model computer code COMPLET. The theoretical results are compared with the experimental excitation functions obtained from EXFOR data source, IAEA. In general the shape of the theoretical excitation functions were fairly reproduced with the experimental results. The study shows that at intermediate energy, alpha induced reactions on medium weight nuclei occurs through pre-equilibrium as well as equilibrium (compound) nucleus stages.

Table of Contents

Table of Contents	vi
List of Figures	vii
Introduction	1
1 Theories of Nuclear Reaction	5
1.1 Wave Mechanical Theory for Single Entrance and Exit Channels . . .	5
1.2 Pre-equilibrium Decay Models	12
1.2.1 Introduction	12
1.2.2 Intra-nuclear Cascade Model	14
1.2.3 The Harp-Miller-Berne(HMB) Model	15
1.2.4 The Exciton Model	17
1.2.5 The Hybrid model	22
1.2.6 The Geometry Dependent Hybrid(GDH) Model	23
1.3 The Compound Nucleus Theory	23
1.4 Direct nuclear reaction	27
2 Computer Code and Formalism	30
2.1 Computer Code COMPLET	30
2.2 Formalism	32
3 Reaction Channels,Analysis and Discussion	36
3.1 Reaction Channels	36
3.2 Analysis and Discussion	40
4 Summary and Conclusion	48
4.1 Summary	48
4.2 Conclusion	49

List of Figures

1.1	Possible values of elastic and reaction scattering cross section.	12
1.2	A crude diagram representing the cascade model	14
1.3	Harp-Miller-Berne model Ref.[4]	15
1.4	physical concept of the exciton model	18
1.5	Interference in direct interaction in the surface of the nucleus Ref[6] .	28
1.6	Direct interaction angular distributions	29
2.1	Energies of excited states for different total angular momentum showing yrast line	35
3.1	Decay scheme of ^{72}As	38
3.2	Decay scheme of ^{71}As	38
3.3	Decay scheme of ^{70}As	39
3.4	Decay scheme of ^{74}As	39
3.5	Experimental and theoretical excitation function for the reaction $^{69}\text{Ga}(\alpha, n)^{72}\text{As}$	43
3.6	Experimental and theoretical excitation function for the reaction $^{69}\text{Ga}(\alpha, 2n)^{71}\text{As}$	44
3.7	Experimental and theoretical excitation function for the reaction $^{69}\text{Ga}(\alpha, 3n)^{70}\text{As}$	44
3.8	Experimental and theoretical excitation function for the reaction $^{69}\text{Ga}(\alpha, p3n)^{69}\text{Ge}$	45
3.9	Experimental and theoretical excitation function for the reaction $^{71}\text{Ga}(\alpha, n)^{74}\text{As}$	45
3.10	Experimental and theoretical excitation function for the reaction $^{71}\text{Ga}(\alpha, 4n)^{71}\text{As}$	46
3.11	Experimental and theoretical excitation function for the reaction $^{71}\text{Ga}(\alpha, n)^{74}\text{As}$ for two exciton numbers.	46

3.12 Experimental and theoretical excitation function for the reaction $^{69}\text{Ga}(\alpha, n)^{72}\text{As}$ for two level density values	47
--	----

Introduction

The study of nuclear reaction is important because it provides knowledge about the nature of nuclear forces, nuclear structure and to explain many other phenomena related to nucleus. Because of this the measurement and calculations of the cross section of nuclear reactions as much accurate as possible and understanding of nuclear reaction mechanisms is an important issue. The shapes of the variation of reaction cross section with excitation energy (excitation function) reveals the reaction mechanisms. The process of production of new nuclei and elementary particles in collision of particles and nuclei is known as nuclear reaction. A general nuclear reaction can be expressed by $X + x \rightarrow Y + y + Q$. Where x is the bombarding particle (projectile), which strike a target X and produce the residual nucleus Y and outgoing particle y. Q is the energy released in the reaction; so that Q is positive for exoergic reactions and negative for endoergic reactions. A nuclear reaction is usually expressed in compact form as X(x, y)Y. The bombarding particle may be a neutron (n), proton (p), deuteron (d) triton (t), alpha-particle or any other heavy ion. The emitted particles may be a nucleon, nucleons, a nucleus or gamma-radiations.

In this thesis the *alpha – particle* is the projectile or the bombarding particle and Gallium isotopes are the targets. The different reaction channels studied are

${}^{69}\text{Ga}(\alpha, n){}^{72}\text{As}$, ${}^{69}\text{Ga}(\alpha, 2n){}^{71}\text{As}$, ${}^{69}\text{Ga}(\alpha, 3n){}^{70}\text{As}$, ${}^{69}\text{Ga}(\alpha, p3n){}^{69}\text{Ge}$, ${}^{71}\text{Ga}(\alpha, n){}^{74}\text{As}$

and ${}^{71}\text{Ga}(\alpha, 4n){}^{71}\text{As}$.

The objective of this thesis is to investigate the mechanisms of alpha-particle induced reaction on gallium isotopes from 10MeV to 70MeV projectile energies with the help of computer code COMPLET. To the best of our knowledge this is done for the first time. The different channels are the results of the projectile energies. For many years it was assumed that all types of nuclear reactions takes place in two stages, a direct stage that occurs in the time it takes a projectile to cross the target nucleus which is about 10^{-21}s and a compound nucleus stage when emission takes place from equilibrated nucleus. Different theories and models that enable the calculations of the cross sections have been developed and used to analyze the experimental data. The direct reaction which includes the 'stripping' and 'pick-up' reactions are characterized by certain angular distributions of the scattered or the outgoing particles. Those particles can be understood by regarding the reactions as having involved only the interaction between the incident particle and the outer nucleons of the target nucleus.

The second stage of nuclear reaction(compound nucleus) is historically proposed by Niles Bohr. The initiation to develop the compound nucleus theory is the problem for resonance peak of nuclear reactions. According to this theory the sharp peak of the reaction cross section is due to the existence of the quasi-stable nuclear state for particular value of resonance energy. When particle x with this resonance energy approaches the target nucleus X, within the range of nuclear forces, a compound nucleus is formed. This compound nucleus will then disintegrate into two or more products Y and y. Thus this type nuclear reaction is regarded as consisting of two successive steps,the formation and the decay stages. More detailed discussion is given in section 1.3.

Another evidence for the compound nucleus theory is the heavy ion induced reaction. Heavy ion induced reactions with projectile energy closed to coulomb barrier are dominated by compound nucleus and direct reactions. As the projectile energy is increased compound nucleus formation is hindered and incomplete fusion starts competing with the complete fusion. More extensive measurements show that some cross sections cannot be explained using the direct and compound reactions models[1]. This shows that particles are emitted after the direct stage but prior to the establishment of statistical equilibrium, which is the compound nucleus stage. This new stage is given a name pre-equilibrium reaction stages. To explain this theory different pre-equilibrium nuclear reaction models have been developed. The first model developed by J.J Griffin was the exciton model [2]. The model was further modified and developed by M.Blan [3] and et al. In the pre-equilibrium theories of nuclear reaction it is assumed that interaction is due to successive nucleon-nucleon interaction in a series of stages. Each interaction produces a particle-hole $p - h$ pair and the particle-hole pair is called an exciton. In the thesis other four related pre-equilibrium models are presented. Certain nuclear reactions can be explained using a quantum mechanical approach provided that the projectile is not a complex particle like heavy ion. The nucleon-induced reaction is discussed with the quantum mechanical approach as an introduction of this thesis. The alpha-particle-induced reaction is a semi classical treatment. That is the angular distributions are treated quantum mechanically and the forward motion classically.

In chapter two of the thesis the computer code COMPLET and the formalism for the code is discussed. COMPLET computer code is among the many computer cods available to compute the pre-equilibrium and equilibrium excitation functions.

Analysis of reaction cross sections as a function of energy (excitation function) for the alpha-particle-induced reaction on gallium isotopes at different channel energies are analyzed from the calculations obtained using the computer code COMPLET. The theoretical results are compared with the experimental data obtained from EXFOR data source, IAEA[5]. These are plotted together for comparison. The last chapter of the thesis is the conclusion and summary part where the main results are discussed and a brief summary is given.

Chapter 1

Theories of Nuclear Reaction

1.1 Wave Mechanical Theory for Single Entrance and Exit Channels

Nuclear reaction cross-sections may be explained using wave mechanical theory under general assumptions[6]. Let us consider a particle approaching a nucleus parallel to the Z-axis with velocity v . This particle can be represented by a plane wave assuming negligible diffraction effects.

$$\psi_{inc} = e^{ikz} \quad (1.1.1)$$

Here the wave amplitude is unity so that there is only one particle per unit volume and in the incident beam there are v particles per unit area per second, where v is the velocity of the incident particle. Since the particles position with respect to x,y axes can not be precisely specified, the angular momentum value of the particle, $l\hbar$ may take any value. To solve this problem the plane waves must be transformed into a superposition of spherical waves each of which represents a particle of definite angular momentum. Let us find an expression for equation (1.1.1) in terms of expansion of partial waves. It can be seen that e^{ikz} is a solution with axial symmetry of the wave equation

$$\nabla^2\psi + k^2\psi = 0 \quad (1.1.2)$$

This equation can be solved in spherical polar coordinates and the solutions with axial symmetry are of the form

$$\psi_l = g_l(r)p_l(\cos\theta) \quad (1.1.3)$$

Where l is an integer $p_l(\cos\theta)$ is a Legendre polynomial and $g_l(r)$ is that solution of the equation

$$\frac{1}{r^2} \frac{d}{dr} r^2 \left(\frac{dg}{dr} \right) + \left(k^2 - \frac{l(l+1)}{r^2} \right) g = 0 \quad (1.1.4)$$

Which is bounded at the origin. The most general solution of equation (1.1.3) is given by

$$\psi = \sum_{l=0}^{\infty} A_l g_l(r) p_l(\cos\theta) \quad (1.1.5)$$

Where A_l are arbitrary constants. The terms in the infinite series are the partial waves. Hence,

$$e^{ikz} = e^{ikr\cos\theta} = \sum_{l=0}^{\infty} A_l g_l(r) p_l(\cos\theta) \quad (1.1.6)$$

Multiplying both sides by $P_l \cos\theta \sin\theta d\theta$ and integrating with the limits from 0 to infinity of equation (1.1.6) and letting $\cos\theta = t$ we get,

$$\int_{-1}^1 e^{ikrt} p_l(t) dt = \frac{2}{2l+1} A_l g_l(r)$$

$$\frac{2}{2l+1}A_l g_l(r) = \frac{1}{ikr}(e^{ikr} - (-1)^l e^{-ikr}) - \frac{1}{ikr} \int_{-1}^1 e^{ikrt} p'(t) dt \quad (1.1.7)$$

The second term of equation (1.1.7) is of the order of $\frac{1}{r^2}$ which may be seen after integration by parts once more. For large value of r, we get

$$\begin{aligned} \frac{2}{2l+1}(A_l g_l(r)) &\sim \frac{1}{ikr}(e^{ikr} - e^{-il\pi} e^{-ikr}) \\ &= \frac{1}{ikr} \left(e^{\frac{il\pi}{2}} [e^{i(kr - \frac{l\pi}{2})} - e^{-i(kr - \frac{l\pi}{2})}] \right) \\ &= \frac{2i^l}{kr} \sin\left(kr - \frac{l\pi}{2}\right) \end{aligned} \quad (1.1.8)$$

Now $g_l(r)$ can be defined completely by requiring that, $A_l = (2l+1)i^l$ Hence,
 $g_l(r) = \frac{1}{kr} \sin\left(kr - \frac{l\pi}{2}\right)$ (1.1.9)

The required expression is then given by

$$e^{ikz} = \sum_{l=0}^{\infty} (2l+1) i^l g_l(r) p_l(\cos\theta) \quad (1.1.10)$$

It can be seen that $g_l(r)$ is a spherical Bessel function with an asymptotic expression.

That is,

$$g_l(r) = \sqrt{\frac{\pi}{2kr}} J_{l+\frac{1}{2}}(kr) \quad (1.1.11)$$

Where the asymptotic form of the spherical Bessel function is expressed as,

$$J_{l+\frac{1}{2}}(kr) = \frac{1}{(2l+1)!!} \sqrt{\frac{2}{\pi}} (kr)^{l+\frac{1}{2}}, r \ll 1$$

$$J_{l+\frac{1}{2}}(kr) = \sqrt{\frac{2}{\pi}} \sin(kr - \frac{l\pi}{2}), r \gg 1. \quad (1.1.12)$$

The incident wave function is then expressed using equation (1.1.11) and equation (1.1.12) as

$$\begin{aligned} \psi_{inc} &= \frac{1}{kr} \sum_{l=0}^{\infty} (2l+1) i^l p_l(\cos\theta) \sin(kr - \frac{l\pi}{2}) \\ &= \frac{1}{kr} \sum_{l=0}^{\infty} (2l+1) i^l p_l(\cos\theta) \left[\frac{e^{i(kr - \frac{l\pi}{2})} - e^{-i(kr - \frac{l\pi}{2})}}{2i} \right] \end{aligned} \quad (1.1.13)$$

From equation (1.1.13), it can be seen that $\frac{1}{r} e^{-i(kr - \frac{l\pi}{2})}$ represents a spherical wave converging (going onto) the nucleus and $\frac{1}{r} e^{+i(kr - \frac{l\pi}{2})}$ represents a spherical wave diverging or going out from the nucleus. If the out going waves are affected in amplitude as well as in phase, we have an inelastic process which can be represented by the wave equation,

$$\psi_l(r) = \frac{1}{2ikr} \sum_{l=0}^{\infty} (2l+1) i^l p_l(\cos\theta) (\eta_l e^{i(kr - \frac{l\pi}{2})} - e^{-i(kr - \frac{l\pi}{2})}) \quad (1.1.14)$$

Where η_l is a complex constant which contains the effects of the scattering center. Its real part gives the change in amplitude and its imaginary part gives the change in phase. η_l can be represented by

$$\eta_l = |\eta_l| e^{2i\delta_l} \quad (1.1.15)$$

The scattered wave is itself the superpositions of partial waves and may be written as

$$\psi_{sc} = \frac{f(\theta)}{r} e^{ikr} \quad (1.1.16)$$

where $f(\theta)$ is the scattering amplitude. Thus the number of particles crossing unit area per second in the scattered beam is given by

$$v |\psi|^2 = v |f(\theta)|^2 d\Omega \quad (1.1.17)$$

Where $d\Omega$ is an element of solid angle. The value for the scattering amplitude $f(\theta)$ is obtained using equation (1.1.14) and equation (1.1.16)

$$f(\theta) = \frac{1}{2ik} \sum_{l=0}^{\infty} (2l+1)(\eta_l - 1) p_l \cos(\theta) \quad (1.1.18)$$

The two types of reactions, elastic and inelastic, may be inferred from the discussion above. For elastic scattering where there is no loss of incident particles $|\eta_l|^2 = 1$. It means there is no change in amplitude between the incident and the scattered wave, which implies no change in the real part of η_l . η_l is now written as $e^{2i\delta_l}$. Then the scattering amplitude is expressed as

$$f(\theta) = \frac{1}{2ikr} \sum_{l=0}^{\infty} (2l+1)(e^{2i\delta_l} - 1) p_l \cos(\theta) \quad (1.1.19)$$

δ_l is the phase shift in the asymptotic form of the partial wave l . For the inelastic reaction $|\eta_l|^2 < 1$, that is there is a change in amplitude and δ_l is complex. The cross section for the scattered particle may be obtained by applying the probability current

density of the scattered wave function ψ_{sc} . The number of scattered particles(N_{sc}) through a solid angle $d\Omega$ is defined as,

$$N_{sc} = \frac{\hbar}{2im} \int_{-\infty}^{\infty} \int_{-\infty}^{\infty} \left(\frac{\partial \psi_{sc}}{\partial r} \psi_{sc}^* - \frac{\partial \psi_{sc}^*}{\partial r} \psi_{sc} \right) r_0^2 d\Omega N_{sc} = v \int \int |f(\theta)|^2 d\Omega \quad (1.1.20)$$

where m is the mass of the scattered particles and r_0^2 is the radius of a sphere with solid angle $d\Omega$. The scattered cross section is given by

$$\begin{aligned} \sigma_{sc} &= \frac{N_{sc}}{Flux} \\ &= \frac{v \int \int |f(\theta)|^2 d\Omega}{v} \\ &= \int \int |f(\theta)|^2 d\Omega \\ &= \sum_{l=0}^{\infty} (2l+1) |1 - \eta_l|^2 \end{aligned} \quad (1.1.21)$$

The reaction cross section may be obtained in the same way but using a negative sign before the probability current to indicate the direction of current onto the nucleus.

$$\sigma_r = \frac{N_r}{v} = \frac{\pi}{k^2} \sum_{l=0}^{\infty} (2l+1) (1 - |\eta_l|^2) \quad (1.1.22)$$

From equation (1.1.22) it is clear that if $|\eta_l| = 0$, that is no change in amplitude of the wave, there is no reaction ($\sigma_r = 0$) but scattering may be there. On the other hand if $\eta_l = 1$, both reaction and scattering are not possible. If $\eta_l = -1$, there is no reaction

but there is maximum scattering. If $\eta_l = 0$, then there is maximum reaction and also some scattering. The total cross section is obtained by adding equation (1.1.21) and equation (1.1.23).

$$\sum_0^{\infty} \sigma_{l,t} = \sum_0^{\infty} \frac{2\pi}{k^2} (2l + 1) (1 - \text{Re} \eta_l)$$

$$\sigma_t = \frac{4\pi}{k^2} \sum_l (2l + 1) \sin^2 \delta_l \quad (1.1.23)$$

These different cases are shown in Fig 1.1.

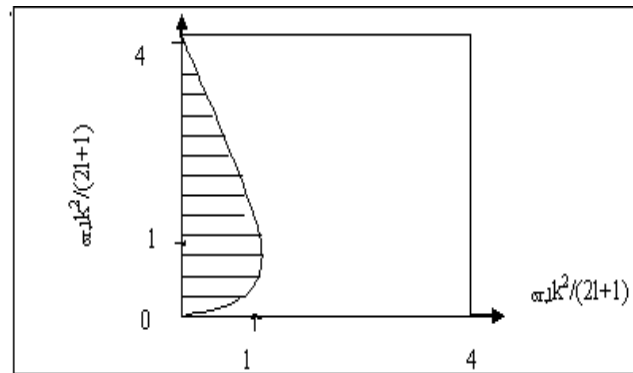


Figure 1.1: Possible values of elastic and reaction scattering cross section.

The shaded region is possible values of the cross section,taken from Ref.[6]

1.2 Pre-equilibrium Decay Models

1.2.1 Introduction

Nuclear reaction mechanisms at intermediate excitation energy is now supposed to proceed through equilibrium as well as pre-equilibrium emission of particles[1],[3]. The high energy tail observed in excitation functions of light charged particles contains important information about the reaction mechanisms. For explaining different observations nuclear physics needs models. The developed models are checked with experimental data to see the extent how much they can reproduce these data.

In this thesis some what five related pre-equilibrium models are presented. First a brief review of the calculation used for high energy 'cascade' reactions commonly known as Intra nuclear cascade calculations is given. This was the earliest type has been tried to answer the question of equilibration. Secondly the model presented by

Harp, Miller and Berne is discussed. In this model the reaction is assumed to proceed by succession of two-body interaction and the nucleon-nucleon scattering cross section are used to compute transition rates. The energy ranges accessible to scattered nucleons are broken into computationally convenient bin size and the occupation number of each bin is followed as a function of time. Thus both particle-hole and energy distributions are explicitly followed as a function of time on an absolute basis. The third model discussed is the Exciton model developed by J.J Griffin[2]. The model treats the equilibration process as proceeding through a sequence of ever more complex intermediate states. Complexity refers to the number of particles and holes or 'exciton' which partition the excitation energy. In this model transitions are assumed to proceed by a residual two-body interactions and an equal a-prior probability for the energy distribution of the exciton of each intermitted state.

The fourth model is the Hybrid model which combines the abilities to calculate the absolute decay and transition rates as in *HMB* model and the exciton model through the use of intermediate state densities. The fifth model discussed is the Geometry-dependent Hybrid model (*GDH*)[3] model. This model tries to introduce the effects of nuclear density distribution into the mentioned pre-equilibrium models. Among these models the Hybrid and the Geometry-dependent Hybrid *GDH* models[1],[3] have been reasonably successful in reproducing a broad range of experimental data. In this thesis these two pre-equilibrium models and the compound nucleus theory and its models are applied to study the α - *particle* induced reaction on gallium isotopes.

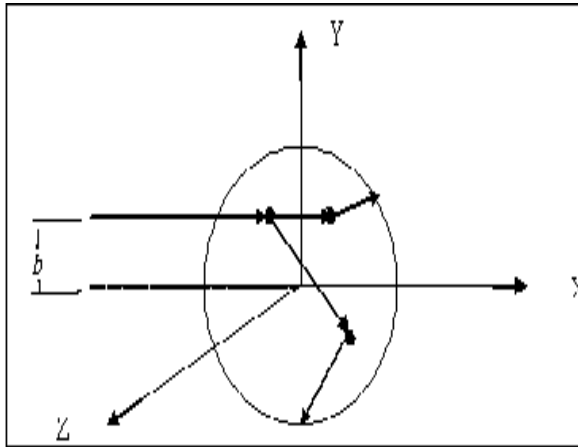


Figure 1.2: A crude diagram representing the cascade model

1.2.2 Intra-nuclear Cascade Model

In the Intra-nuclear cascade model the projectile enters the target nucleus with a given impact parameter 'b' after traveling a certain distance, it interacts with the target nucleon and excites it above the Fermi sea. The scattered particles then travel through the nucleus interacting with the other nucleons. The Intra-nuclear cascade model traces the individual nucleon trajectory in three-dimensional geometry. Particles reaching the nuclear surface with sufficient energy to be emitted are assumed to be emitted. A crude diagrammatic representation of the cascade model is shown in Fig.1.2 where the succession of two-body interaction is followed in three-dimensional geometry.

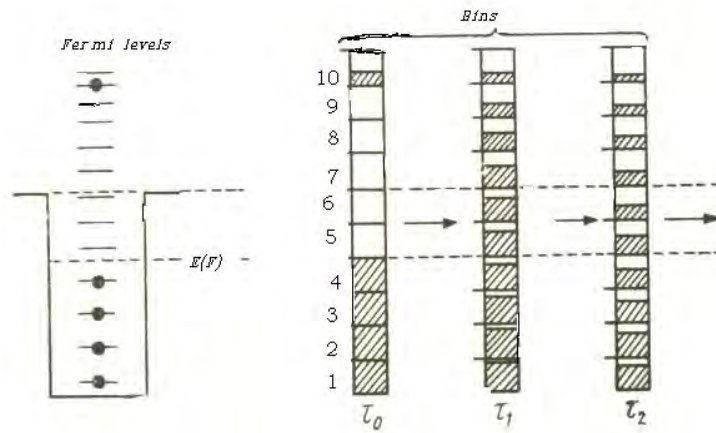


Figure 1.3: Harp-Miller-Berne model Ref.[4]

1.2.3 The Harp-Miller-Berne(HMB) Model

In this model the nuclear single particle states are classified according to their energies in groups or bins whose size $\Delta\epsilon$ is chosen to be some convenient dimension, say 1MeV. The number of available single particle levels in each bin are computed. A Fermi gas distribution has been used in calculations. The calculation can be applied either beginning with some initial arbitrary population of excited particles and holes or with nucleus. The physical idea of the HMB model [4], is illustrated in Fig. 1.3.

The fractional occupation of each bin is followed in the calculation as a function of time using a Fermi distribution. At the initiation of the reaction when the time is τ_0 all the levels below the Fermi energy are filled up (as the target is in the ground state) and the projectile is in an excited state. This gives the fractional occupation probability at the time $\tau = \tau_0$. After the two-body interaction a redistribution of probabilities occur as shown in Fig.(1.3).

After computing the relative probabilities of scattering into and out of each bin

and of emission from bins above the particle binding energy, populations of all bins are changed accordingly. Again for the particles occupying each bin the earlier calculations is repeated so that all possible ways of scattering into and out of each bin must be computed and the populations are changed accordingly. The solution of the equilibration process in this model rests in computer solution of a set of coupled differential equations. The advantages of this model are the use of nucleon-nucleon scattering approach for each transition to generate transition rates on absolute basis.

1.2.4 The Exciton Model

The Exciton model proposed by J.J Griffin[2] has been used to calculate the energy distribution of emitted particles. As the pre-equilibrium nuclear reactions follow the excitation process which take place by successive nucleon-nucleon interactions in a series of stages, it is taken that each interaction produces particle-hole ($p - h$) pair or exciton. Usually each nucleon-nucleon interaction produces another exciton but occasionally a particle receive enough energy for it to be emitted. The energy distribution of these pre-equilibrium particles changes as the reaction proceeds. Those emitted in the earlier stages have, on average, more energy than those emitted in the latter stages. The physical concept of the exciton model is illustrated in Fig.1.4.

A nucleon is shown entering the nuclear potential on the left. The projectile nucleon interacts with the target nucleons with a given energy and form a one particle zero hole ($1p0h$) state, that is a state with exciton number $n = 1$. At this stage the projectile has entered the nuclear force field but has not been absorbed by the target. Since all the levels below the Fermi energy are filled, the first interaction between the projectile and the target nucleon will lead to a $2p1h$ (two particle and one hole) which leads to a formation of $n = 3$ exciton state. After the formation of $n = 3$ state either of the excited particles may be emitted if it has sufficient energy to escape. On the other hand if particle emission does not take place, then there will be a further two-body interaction between one of the two excited particles and a particle below the Fermi level or between the two excited particles themselves. The former leads to the formation of $n = 5$ exciton state ($3p2h$) while the latter leads to a new $n = 3$ exciton state having different energy configurations of particles and holes or back to the original $n = 1$ state.

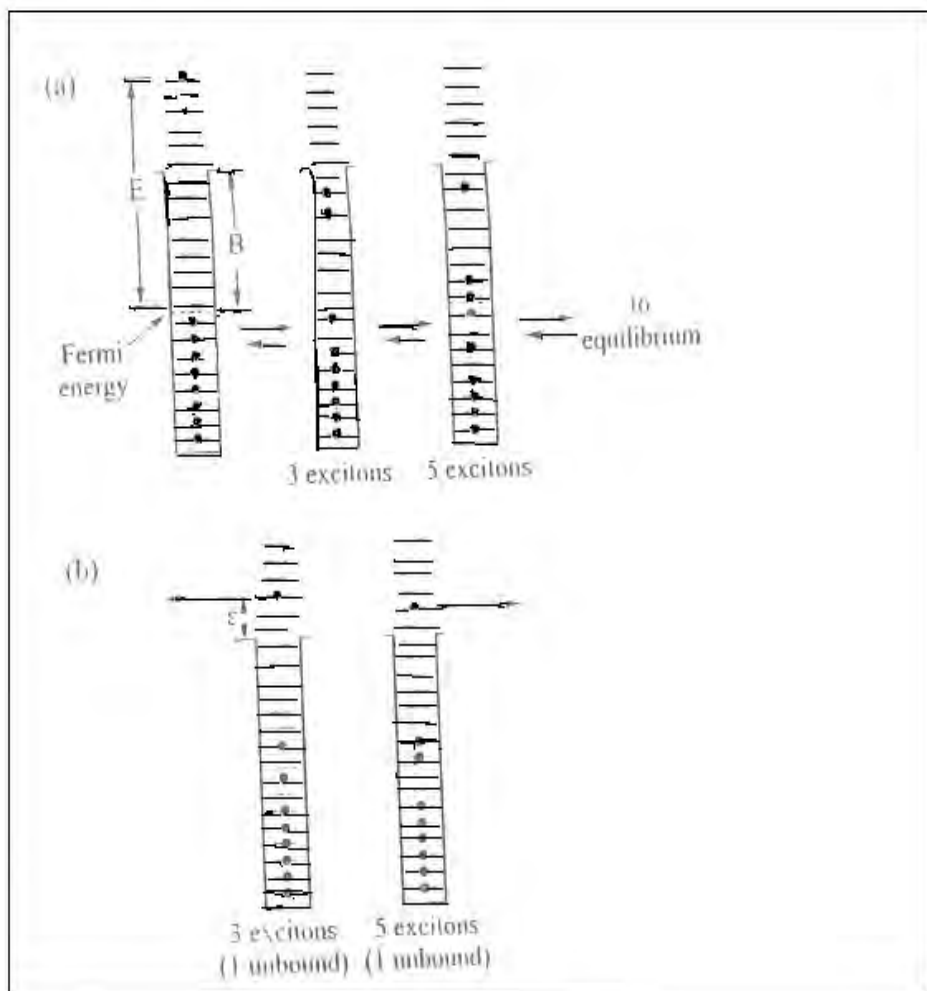


Figure 1.4: physical concept of the exciton model

The two-body interaction then leads to the transitions in which the change in exciton number is

$$\Delta n = \pm 2, 0 \quad (1.2.1)$$

The exciton level density, which is the intermediate state density, plays an important role in the exciton model. The single particle level densities are often used to calculate the exciton level densities, assuming the nucleus to be degenerate Fermi gas with equidistant spacing (levels) [7]. The transition rates are proportional to the level density of the final accessible states (Fermi golden rule). Ericson [3] derived a simple expression for the partial level density, that is level density of the exciton state n of a nucleus with excitation energy E .

$$\rho_n(E) = \frac{g(gE)^{n-1}}{p!h!(n-1)!} \quad (1.2.2)$$

where g is the single particle level density which is expressed in terms of the single particle spacing d , as $g = \frac{1}{d}$ and p and h are the number of excited particles and holes respectively. Taking Pauli's principle into consideration PE Hodgson [7] gave another expression for particle-hole density in equidistant spacing model.

$$\rho_n(E) = \frac{g(gE - A(p, h))^{n-1}}{p!h!(n-1)!} \quad (1.2.3)$$

where $A(p, h) = \frac{1}{4}(p^2 + h^2 + p - h) - \frac{1}{2}h$ and $n = p + h$. The decay probability from an n exciton state $P_n(\epsilon)$ is defined as the ration of the emission rate from n to the states of all transitions including emission from n . If $\lambda^n(\epsilon)$ be the emission rate with energy

ϵ from n exciton state and λ_+^n, λ_-^n and λ_0^n are the rates of $\Delta n = 2, -2, 0$ transitions respectively, then the decay probability becomes;

$$P_n(\epsilon) = \frac{\lambda^n(\epsilon)}{\lambda_+^n + \lambda_-^n + \lambda_0^n + \int d\epsilon \lambda^n(\epsilon)} \quad (1.2.4)$$

The emission rates as obtained from the principle of detailed balance assuming constant transition time (τ_n) as obtained by Williams [3] is

$$\lambda^n(E) = \frac{(2s+1)}{\pi^2 \hbar^2} \left(\frac{\rho_{n\ell}(U)}{\rho_{n\ell}(E)} \right) m \epsilon \sigma_{inv}(\epsilon) \quad (1.2.5)$$

Where s and m are the intrinsic spin and reduced mass of the ejectile, $n\ell$ is the exciton number after emission of ejectile with ν nucleons, $n\ell = n - \nu$. U is the residual excitation energy which is, $U = E - B - \epsilon$, with B the ejectile binding energy. $\sigma_{inv}(\epsilon)$ is the inverse cross section. For several g values of excitations, it can be seen from equation (1.2.5) that $\lambda^n(E)$ is rapidly increasing function of n when $n \ll \bar{n}$ [1],[7]. With the assumption that for $n \ll \bar{n}$, *Griffin*[2] presented a model derivation for which only transitions with $\Delta n = +2$ are considered and $\Delta n = 0, -2$ transitions can be neglected. It is assumed that the fraction of n -exciton states in which one particle is at an energy $\epsilon + B$ above the Fermi energy is given by the ratio, $\frac{\rho_n(U, \epsilon)}{\rho_n(E)}$, where U is the residual particle excitation energy if there is particle emission with channel energy ϵ . The other quantity $\rho_n(U, \epsilon)$ is the density of states with n -exciton one of which has an energy such that if emitted the residual nucleus would have excitation U and the particle channel energy ϵ . $\rho(E)$ is density of states having n excited particles and holes at excitation energy E . The individual transition rates $\lambda^{n\pm,0}$ are obtained using Fermi golden rule and are defined as

$$\lambda_+^n = \frac{2\pi}{\hbar} |M_+|^2 \rho_{n+2} \quad (1.2.6)$$

$$\lambda_-^n = \frac{2\pi}{\hbar} |M_-|^2 \rho_{n-2} \quad (1.2.7)$$

$$\lambda_0^n = \frac{2\pi}{\hbar} |M_0|^2 \rho_n \quad (1.2.8)$$

where M_+ , M_- , and M_0 are the matrix elements of the respective transitions, ρ_{n+2} , ρ_{n-2} and ρ_n are the density of states available in $n+2$, $n-2$ and n exciton states after $\Delta n = 2, -2, 0$ transitions. With an implicit assumptions that the mean life time τ_n of the n -exciton state is constant which leads $M_+ = M_- = M_0$ the transition rates were given by Williams [3]

$$\lambda_+^n = \frac{2\pi}{\hbar} |M|^2 \frac{g^3 U^2}{2(p+h+1)} \quad (1.2.9)$$

$$\lambda_-^n = \frac{2\pi}{\hbar} |M|^2 \frac{gph(p+h-2)}{2} \quad (1.2.10)$$

$$\lambda_0^n = \frac{2\pi}{\hbar} |M|^2 g^2 U \left[\frac{3(p+h)-2}{4} \right] \quad (1.2.11)$$

The matrix element is evaluated empirically .The most common form of $|M|^2$ empirical results for nucleon-nucleon scattering is given by Kalbach [1].

$$|M|^2 = \frac{k \sqrt{\frac{e}{7\text{Mev}}} \sqrt{\frac{e}{2\text{Mev}}}}{eA^3} \quad (1.2.12)$$

for $e < 2 \text{ Mev}$

$$|M|^2 = \frac{k\sqrt{\frac{e}{7\text{Mev}}}}{eA^3} \quad (1.2.13)$$

for $2 \text{ Mev} \leq e \leq 7 \text{ Mev}$

$$|M|^2 = \frac{k\sqrt{\frac{15\text{Mev}}{e}}}{eA^3} \quad (1.2.14)$$

for $e \geq 15 \text{ Mev}$

where $e = \frac{E}{n}$ and $k = 135\text{Mev}^3$.

1.2.5 The Hybrid model

The Hybrid model was proposed by Blann [3]. The model uses the approach which is designed to have the physical transparency and simplicity of the exciton model while permitting the calculation of absolute spectral yields as in the *HMB* model. Since the idea is borrowed from both models *Blann* called this model the Hybrid model. The Hybrid model uses nucleon-nucleon scattering cross section to calculate absolute spectral yields as was in the cascade and *HMB* models. Blann gave the empirical expression for the two-body interaction rates λ_{n+2} from free nucleon-nucleon scattering cross sections [3]. The internal transition rates of an excited particles at energy $\epsilon + B$ above the Fermi energy for energies below 100 MeV is represented by

$$\lambda_{n+2}(\epsilon) = [1.4 \times 10^{21}(\epsilon + B) - 6.0 \times 10^{18}(\epsilon + B)]k^{-1} \quad (1.2.15)$$

where $\lambda_{n+2}(\epsilon)$ represents the rate at which a nucleon at a given energy $\epsilon + B$ above the Fermi energy undergoes two-body interactions, B is the separation energy and k^{-1} is an adjustable constant, $k = 1$, gives a result for nuclear matter of average interior density.

1.2.6 The Geometry Dependent Hybrid(GDH) Model

The nucleon density distribution in the nuclear skin can affect the pre-equilibrium decay in two ways. First the mean free path in the intranuclear transitions is greater in the diffused edges and secondly the Fermi energy will be lower in that region so that the hole depth is limited. Considering these effects the Hybrid model for the cross sections was reformulated as a sum of contributions over impact parameter [1],[3].

$$\sigma_{\nu}(\epsilon)d\epsilon = \frac{\pi}{k^2} \sum_{l=0}^{\infty} (2l+1) T_l P_{\nu}(\epsilon) d\epsilon \quad (1.2.16)$$

Where $P_{\nu}(\epsilon)$ is the pre-equilibrium decay probability calculated as a function of nuclear density and T_l is the transmission coefficient. For the calculation of the nuclear density the Fermi distribution may be applied as used by M. Blann [3].

$$d(R) = \frac{\bar{d}}{[e^{\frac{R-c}{z}} + 1]} \quad (1.2.17)$$

Where $d(R)$ is the nuclear matter density at radius R , \bar{d} is the central nuclear density, $c = 1.07 A^{\frac{1}{3}}$ fm and $z = .55$ fm. The transition rates in the Hybrid model in each region is multiplied by $\frac{\bar{d}}{\langle d(R) \rangle}$ to include all impact parameters. Where $\langle d(R) \rangle$ represent the average density for the impact parameter taken into consideration.

1.3 The Compound Nucleus Theory

Niles Bhor(1936)[8] pointed out that nuclear reaction of a certain type undergoes in two stages, the capture of incident particle (projectile) by the target nucleus to form a compound nucleus and the decay of the compound nucleus, thus a nuclear reaction of this type is described as $x + X \rightarrow C^* \rightarrow Y + y$.

Bohr postulated that the energy of the incident particles rapidly shared between all the nucleons of the system until sufficient energy is concentrated on a nucleon or a group of nucleons that the compound nucleus can decay by the emission of these particles. On nuclear time scale this takes a considerable time, which is about $(10^{-13} - 10^{-16} \text{ s})$. Thus the compound nucleus forgets its history of formation by the time it decays. That is the decay of the compound nucleus depends only on its energy (E_c), angular momentum and parity but not on its particular mode of formation. The cross section for such nuclear reaction is given by

$$\sigma(\alpha, \beta) = \sigma_c(\alpha)G_c(\beta) \quad (1.3.1)$$

Where $\sigma_c(\alpha)$ is the cross section for the formation of the compound nucleus (C) through channel α and $G_c(\beta)$ is the probability that C will decay through channel β . For the matter of simplicity if the dependence of $G_c(\beta)$ on angular momentum and parity is neglected $G_c(\beta)$ will be a simple energy dependent quantity. From the uncertainty in E_c of a decaying state its width is given by

$$\Gamma_\beta(E_c) = \frac{\hbar}{\tau_\beta} \quad (1.3.2)$$

The total decay probability (Γ) of the compound nucleus is obtained by summing equation (1.3.2) over all channels. As $G_c(\beta)$ is the probability that a compound nucleus decay through channel β , it can be expressed as

$$G_C(\beta) = \frac{\Gamma_\beta(E_c)}{\Gamma(E_c)} \quad (1.3.3)$$

By the reciprocity theorem the reaction cross section $\sigma(\alpha, \beta)$ and $\sigma(\beta, \alpha)$ are related as

$$k_{\alpha}^2 \sigma(\alpha, \beta) = k_{\beta}^2 \sigma(\beta, \alpha) \quad (1.3.4)$$

Where $\sigma(\alpha, \beta)$ is the cross section with entrance channel α and reaction channel β and $\sigma(\beta, \alpha)$ is the inverse cross section. If equation (1.3.1) and equation (1.3.3) are substituted in equation (1.3.4), we get an important relation.

$$\frac{k_{\alpha}^2 \sigma_c(\alpha)}{\Gamma_{\alpha}(E_c)} = \frac{k_{\beta}^2 \sigma_c(\beta)}{\Gamma_{\beta}(E_c)} = U(E_c) \quad (1.3.5)$$

Where $U(E_c)$ is a function depending only on E_c but not on a particular channel used. The probability that a compound nucleus decay through a given channel is obtained by combining equation (1.3.4) and (1.3.6)

$$G_c(\beta) = \frac{k^2(\beta)}{\sum_{\Gamma} k_{\gamma}^2 \sigma_c(\gamma)} \quad (1.3.6)$$

This last equation tells that, if the compound nucleus formation cross section through all possible channels is known then it is possible to obtain the decay probability through a given channel.

Combining equations (1.3.1) and (1.3.6) the cross-section becomes

$$\sigma(\alpha, \beta) = \frac{\sigma(\gamma) k_{\beta}^2 \sigma(\beta)}{\sum_{\gamma} k_{\gamma}^2 \sigma(\gamma)} \quad (1.3.7)$$

Ejectiles with energy range ϵ_{β} to $\epsilon_{\beta} + d\epsilon_{\beta}$ leave the residual nucleus with energy in the range U_{β} to $U_{\beta} + dU_{\beta}$, where $U_{\beta} = E_{CN} - B_{\beta} - \epsilon_{\beta}$, E_{CN} and B_{β} are respectively the compound nucleus energy and the binding energy of the ejectile. Introducing the density of levels $\rho(U_{\beta})$ of the residual nucleus and statistical weights g_{β} and g_{α}

through the two channels, the angle integrated cross-section becomes

$$\sigma(\alpha, \beta)d\epsilon_\beta = \frac{\sigma(\gamma)g_\beta k_\beta^2 \sigma(\beta)\rho(U_\beta)dU_\beta}{\sum_\gamma \int_0^{\epsilon_{max}} g_\gamma k_\gamma^2 \sigma(\gamma)\rho(U_\gamma)dU_\gamma} \quad (1.3.8)$$

Since $k^2 = 2mE$, m the reduced mass of the ejectile, the above equation is reduced to

$$\sigma(\alpha, \beta)d\epsilon_\beta = \frac{\sigma(\gamma)(2I_\beta + 1)m_\beta \epsilon_\beta \sigma(\beta)\omega(U_\beta)dU_\beta}{\sum_\gamma \int_0^{\epsilon_{max}} (2I_\gamma + 1)m_\gamma \epsilon_\gamma \sigma(\gamma)\omega(U_\gamma)dU_\gamma} \quad (1.3.9)$$

This last equation is known as the Weisskopf-Ewing formula for the angle integrated cross-section. To a good approximation, the level density $\rho(U)$ can be shown to be proportional to $\exp(\frac{U}{T})$, so that the ejectile spectrum given by the Weisskopf-Ewing theory is Maxwellian.

1.4 Direct nuclear reaction

A nuclear reaction may take place only with certain parts of the target nucleus being the rest remains undisturbed. One property which distinguishes this type of reaction, direct reaction, from the compound nucleus reaction is that it proceeds much more rapidly, in time of the order of the nuclear transit time about 10^{-21} . Unlike compound nucleus theory, experiments show that the differential cross section of certain type of reaction is strongly peaked in the forward direction. This may be accounted for if it is assumed that some of the incident particles interact with nucleons in the equatorial rim of the target nucleus. In doing so they lose some energy and are deflected through a small angle but not captured into the compound nucleus. When the incident particles are positively charged, some of them which also interact with the interior of the nucleus will be reflected back by the Coulomb barrier until they are captured into the compound nucleus [7]. However, this compound nucleus will decay predominantly through the emission of neutron, so that the compound process is dominant in the (p,n) reaction. Therefore at energies in tenths of MeV region, compound nucleus formation is one of the several competing processes and the direct reaction may be able to yield information about some regions of the nucleus participating reactions. A direct interaction may be described by means of a semi-classical approach to visualize the process. If we take the target nucleus to be moderately absorptive so that direct reaction takes place throughout the nuclear surface, the interference in the surface of the nucleus may be studied with a simple geometrical representation.

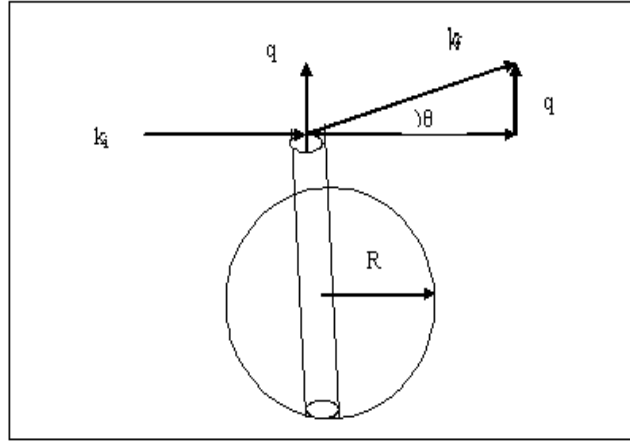


Figure 1.5: Interference in direct interaction in the surface of the nucleus Ref[6]

Let the wave vectors of the incident and the scattered particles be k_i and k_f then the angular momentum transfer is given by $l = (k_i - k_f) \times r = q \times r$ where r is the position vector at the point of interaction of the incident and the target particle(nucleons) and q is the linear momentum transfer in units of \hbar . The locus of the point of interaction for a given l and q is the surface of the cylinder of radius $\frac{l}{q}$ with its axis in the direction of q . Expressing q in terms of the scattering angle θ , we get

$$q = \sqrt{[k_i^2 + k_f^2 - 2k_i k_f \cos\theta]} \quad (1.4.1)$$

The cosine of the angle made by the scattering particle from its initial direction is then given by the equation

$$\cos\theta = \frac{k_p^2 + k_d^2}{2k_p k_d} - \frac{l^2}{2k_p k_d R^2} \quad (1.4.2)$$

If the scattering from the interior of the nucleus is ignored, then the scattering into the angle θ due to the partial wave is the result of an interference from the

two ends of the cylinder when they enter the surface region of the nucleus. Because of the interference from opposite sides of the nucleus, the differential cross section will exhibit a diffraction pattern. Further more for the excitation of low lying states in a direct reaction, the struck nucleon must receive little energy and hence little momentum ($k_i \sim k_f$), so that q is small. Hence scattering will be largely in the forward direction. On the other hand for $\frac{l}{q} > R$, there will be little interaction, since the cylinder only intersects a narrow rim of the nuclear surface. Thus, for $l = 0$ scattering into very small region is inhibited and the larger l the larger is the angle at which the first scattering maximum occurs. The scattering cross-section is found to be proportional to the modules square of spherical Bessel's function [8]. Some direct interaction angular distributions are shown in Fig.(1.6) taken from Ref.[6].

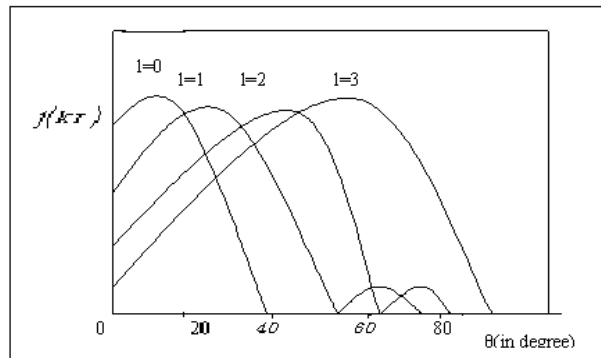


Figure 1.6: Direct interaction angular distributions

In the above Fig. each l - value has to be multiplied by a factor of 1, 0.1, 0.06, 0.02 respectively.

Chapter 2

Computer Code and Formalism

2.1 Computer Code COMPLET

The code COMPLET is based on same philosophy as the former code INDEX[9]. It applies the statistical model of compound nucleus decay developed by Weisskopf-Ewing [10] and the hybrid and geometry-dependent hybrid model of Blann [3] and the further simplification and improvement by J.Ernst [11]. It predicts the yield of residual nuclei in nuclear reaction with excitation energy up to 225Mev taking into account two mechanisms. The first one,pre-equilibrium emission is accompanied in the frames of the model of independently interacting excitons. For this simplifying assumptions have been made.

- ⊙ The pre-equilibrium emission of complex particles is neglected
- ⊙ The equilibrium is reached after the second stage of evolution and
- ⊙ Maximum two pre-equilibrium nucleons can be emitted.

An approximation concerning pre-equilibrium angular momentum removal is included. The equilibrium part formerly based on Weisskopf-Ewing evaporation formula is also modified to include full angular momentum decoupling regarding emission of

light particles with $A \leq 4$. In COMPLET code a pre-equilibrium process in two stages is assumed. The particles in the initial configuration ($n_0 = EX1 + EX2 + EX3$) can be neutron, proton or alpha particle, represented by the exciton numbers EX1, EX2 and EX3 respectively. It is customary to use the initial exciton number n_0 separated into proton and neutron above and holes below the Fermi level as a fit parameter to match theoretical predictions with experimental excitation functions. The exciton number governs the cascading process of the binary collisions. A good guess would be the number of nucleons in the projectile. On this basis, the theoretical calculations in this thesis is done using $n_0 = 4(2p + 2n + 0h)$. These excitons interact independently with the particles below the Fermi level, creating new particle-hole configuration in the second stage or getting emitted into the continuum. In these interactions the original exciton type is assumed to be conserved. The newly created exciton may be α - particle, α - hole state formed with a probability $(1 - ALF)$. The value of $ALF = 0.2$ is found to be the best choice. Each emitted pre-equilibrium particle x of kinetic energy E_x carries away the angular momentum L with $L = 0.219 \sqrt{\left[\frac{E_x A_x (A - A_x)}{A} \right]}$ is the center of mass wave number of the ejectile and $R = 1.55 A^{3/4} C_{ANG}$ [9]. The coefficient C_{ANG} has nonzero value ≤ 1 . Thus the quantity C_{ANG} adjusts the magnitude of the angular momentum removal. The code COMPLET allows the evaporation of proton, neutron, deuteron and alpha particles, triton and Helium-3. The code COMPLET includes pre-equilibrium proton, neutron and alpha emission up to two particles. The other modification of the code COMPLET is the use of additional parameters such as the rotational energy fission barriers (ROTFAC) and Nuclear friction parameters for the heavy-ion reactions.

The Q-value for the formation of the compound nucleus and the emitted nucleons binding energies in the evaporation chain have been calculated using Myers and Swiatecki mass formula [9]. The mean free-path multiplier for intranuclear transition rates are calculated from optical potential parameters.

2.2 Formalism

In the pre-equilibrium emission calculations, the initial exciton configurations and level density parameters are very essential quantity. The nuclear level density influences the shape and the height of the calculated excitation functions. The level densities of the nuclide involved in the evaporation chain may be calculated from the Fermi density distribution [12].

$$\rho(E) = \frac{\pi^{\frac{1}{2}} e^{2\sqrt{aE}}}{12a^{\frac{1}{4}} E^{\frac{5}{4}}} \quad (2.2.1)$$

Where E is the excitation energy and 'a' the level density parameter. The level density parameter obtained by experiment shows a linear dependent with the mass number of the compound nucleus. In general it is given by an expression,

$$a = \frac{ACN}{K} \quad (2.2.2)$$

Where 'ACN' is the mass of the compound nucleus and the free constant has value which ranges from 7.5-8 [12]. In the thesis the level density parameter 9 is used for both isotopes, which is the best fit to experimental results.

The symmetry energy term may be calculated using the Fermi gas model. The partition of a given nucleons of 'A' into levels is governed by Pauli principle. The symmetric distribution, $Z = A - Z = A/2$, proves to be energetically more favored. Any other repartition, $N = (A/2) + \nu$ or $Z = (A/2) - \nu$ will involve lifting particles from occupied into unoccupied levels. The proton and neutron energy due to symmetry effect using the Fermi gas model is given by

$$E_p = \frac{3}{2} Z E_F \quad (2.2.3)$$

$$E_N = \frac{3}{2} (A - Z) E_F \quad (2.2.4)$$

The pairing energy is to be zero for even-even nucleon, $-\delta$ for odd-even nucleon and $-\delta$ for odd-odd nucleon, with $\delta = \frac{11}{\sqrt{A}}[1]$. Every emitted pre-equilibrium particle of kinetic energy E_x carries away angular momentum $L = k_x R$, where k_x is the wave number of the ejectile and R the radius of the target nucleus. In a classical description in terms of the particle trajectories, R may be interpreted as the most probable distance from the center of the nucleus at which the particle leaves the nucleus. Even though there is a decrease in angular momentum due to the emitted particles, as the projectile energy increases, the nuclear spin of the compound nucleus increases. Increasing the nuclear spin results in increasing the probability of interacting particles to be emitted to a higher levels rather than to be emitted. The rotational energy of the nucleus may be calculated using the rigid body moment of inertia or using the rotating liquid model moment of inertia. The excitation energies of low lying states of even-even nucleus using a quantum-mechanical rigid rotator are given by [11]

$$E = \frac{\hbar^2}{2I} J(J+1) + \alpha J^2(J+1)^2 \quad (2.2.5)$$

Where J is the total angular momentum of the nucleus.

I - the moment of inertia of a quantum-mechanical rigid rotator.

α - is the stretching factor for the rigid rotator as the velocity increases which increases the moment of inertia(I). It is an experimentally determined constant. The classical moment of inertia, to the lowest order in β , for a uniform ellipsoid shape of a nucleus with its two axis equal is given by

$$I = \frac{2}{5} AMR_0^2(1 + 0.31\beta) \quad (2.2.6)$$

Determining β numerically, the moment of inertia(I) and hence the rotational energy can be determined. It can be seen that as the angular momentum increases the energies of the nuclear states increases rapidly. These increased states due to this effect are known as the yrast states. The locus obtained by plotting the variation of the energies of these states with angular momentum is called the yrast line. Yrast states are important in nuclear reaction that at the end of a sequence of particle emissions a gamma-ray cascade takes place down the yrast line. This is because the emission of gamma-ray does not change the nucleus angular momentum.

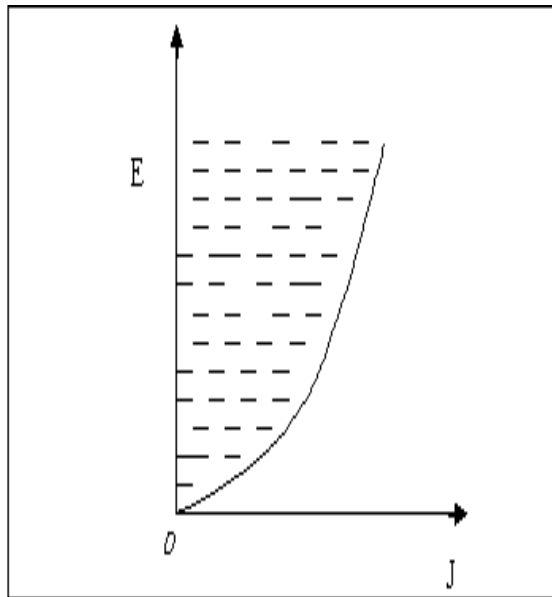


Figure 2.1: Energies of excited states for different total angular momentum showing yrast line

Chapter 3

Reaction Channels, Analysis and Discussion

3.1 Reaction Channels

The target Gallium has two isotopes, ^{69}Ga of natural abundance 60.1% and ^{71}Ga , natural abundance, 39.9%. The theoretical calculations of excitation function are then done separately for these two isotopes. The reaction channel $^{69}\text{Ga}(\alpha, n)^{72}\text{As}$ is obtained by the emission of one neutron from the composite nucleus $^{73}\text{As}^*$. The evaporation residue nucleus ^{72}As is unstable. It has a half-life of $T_{\frac{1}{2}} = 26h$ and decays by electron capture (E.C) (21.1%) and β^+ (78.79%) emission to ^{72}Ge . The spin- parity of the residual nucleus is 2^- .

The $^{69}\text{Ga}(\alpha, 2n)^{71}\text{As}$ reaction channel is the result of emission of two neutrons from the composite nucleus $^{73}\text{As}^*$. The evaporation residue is a radioactive nucleus and decays to ^{71}Ge by E.C (58%) and β^+ (42%) emission. The life time of the residual

nucleus is 62h and its spin parity is $\frac{5}{2}^-$.

The other reaction channel ${}^{69}\text{Ga}(\alpha, 3n){}^{70}\text{As}$ is obtained by evaporation of three neutrons from the compound nucleus. The residual nucleus is unstable and decays to ${}^{70}\text{Ge}$ with half-life of $T_{\frac{1}{2}} = 52m$. The decay is mainly by β^+ (90.8%) and also by E.C(8.2%). The spin parity of the residual nucleus ${}^{70}\text{As}$ is $\frac{9}{2}^+$.

The reaction channel ${}^{69}\text{Ga}(\alpha, p3n){}^{69}\text{Ge}$ is obtained by the emission of three neutrons and one proton from the compound nucleus. The other reaction channel ${}^{71}\text{Ga}(\alpha, n){}^{71}\text{As}$ is formed by the evaporation of one neutron from the compound nucleus ${}^{75}\text{As}$.

The evaporation residue ${}^{74}\text{As}$ is unstable and decays to ${}^{74}\text{Ge}$ with a half-life of 17.5d. The spin parity of ${}^{74}\text{Ge}$ is 2^- . The evaporation residue decays into a stable ${}^{74}\text{Se}$ by emission of β^+ (32%) and ${}^{74}\text{Ge}$ E.C(41%), β^+ (27%).

The last reaction channel ${}^{71}\text{Ga}(\alpha, 4n){}^{71}\text{As}$ is the result of emission of four neutrons from the compound nucleus formed. The decay schemes of the different reaction channels is given from Fig.(3.1) -(3.4)

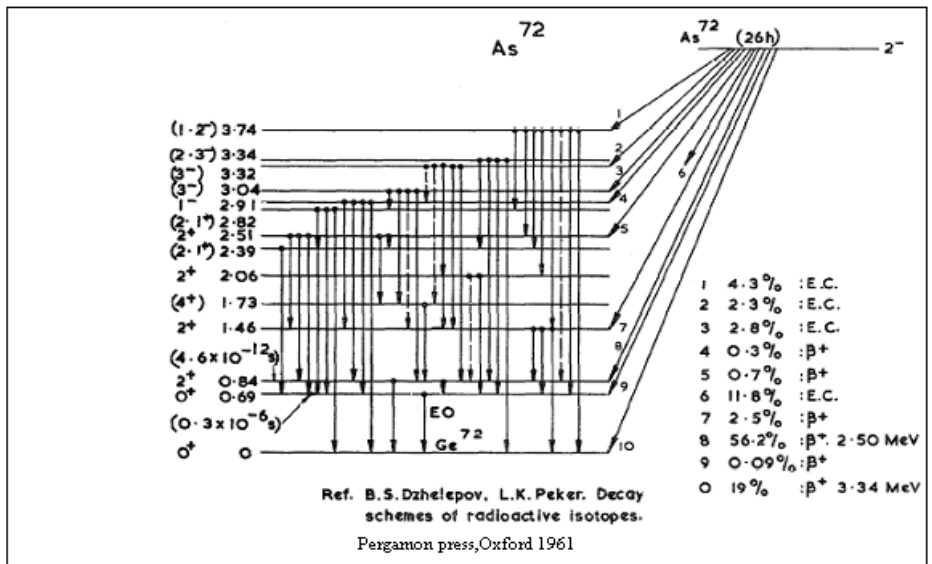


Figure 3.1: Decay scheme of ^{72}As

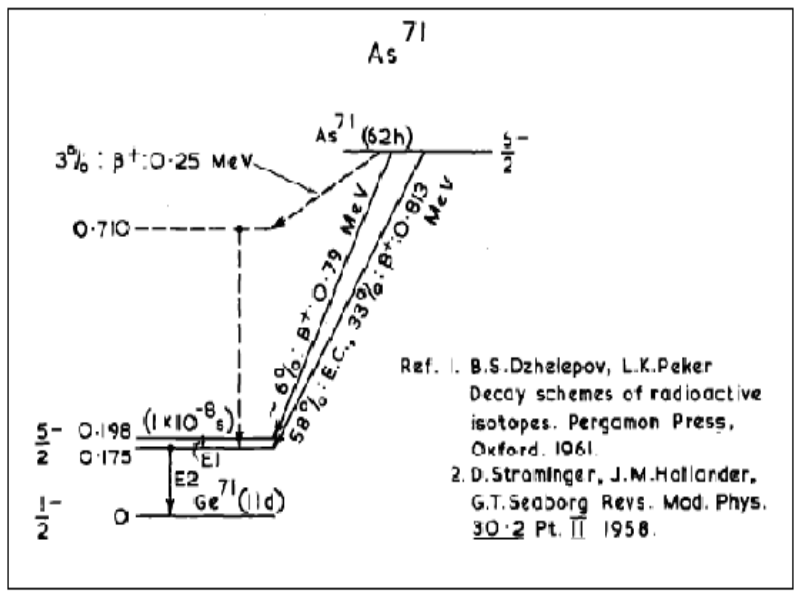
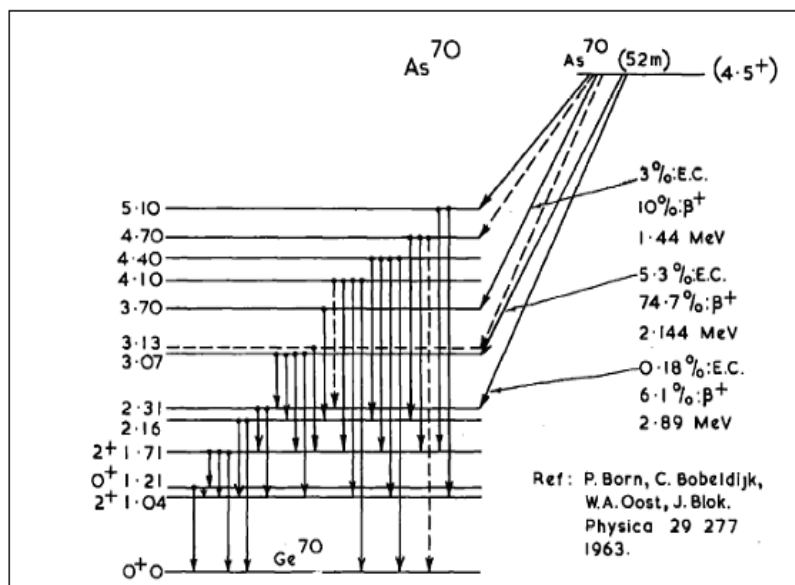
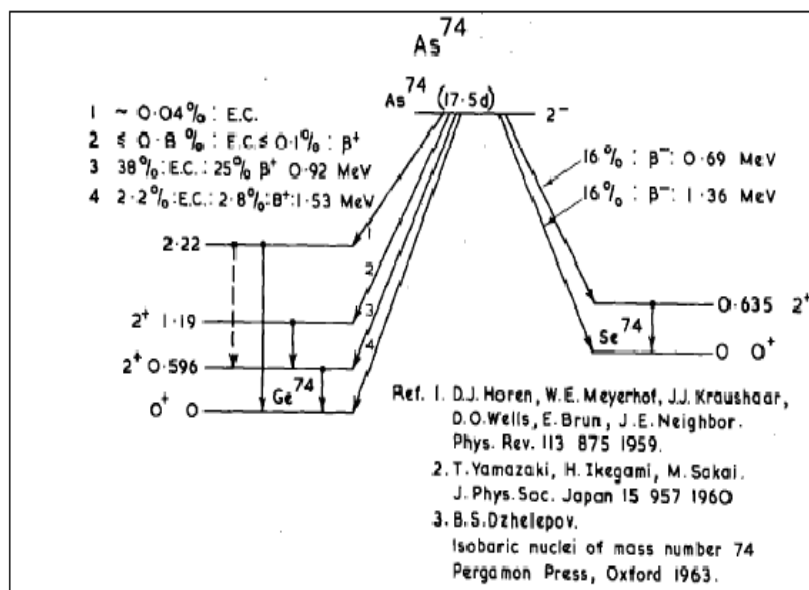


Figure 3.2: Decay scheme of ^{71}As

Figure 3.3: Decay scheme of ^{70}As Figure 3.4: Decay scheme of ^{74}As

3.2 Analysis and Discussion

The excitation function of alpha-particle induced reaction on the two gallium isotopes ^{69}Ga and ^{71}Ga are theoretically evaluated using computer code COMPLET. This code is an extension of the code ALICE-91 and INDEX[9]. These two codes employ the Weisskopf-Ewing model for the statistical part and geometry dependent hybrid model of M.Blann for the pre-equilibrium emission. The code COMPLET considers the approximate pre-equilibrium angular momentum removal for its pre-equilibrium calculations. The equilibrium part which was based on the Weisskopf-Ewing evaporation formula is also modified to include full angular momentum decoupling for light particle evaporation. The $(2s+1)$ multiplicities of the spin s of the ejectiles are taken into account. A simple spin decoupling scheme is used in counting the ways the residual nucleus with spin J' can be reached from the compound nucleus with spin J for all combinations $|J - J'| \leq 12$. Spin dependent level densities are used where the rotational energy according to the liquid drop model is subtracted from the total excitation energy[12]. Pre-equilibrium and equilibrium gamma emission may also be handled by the code. The Q-values are calculated from Myers-Swiatecki mass formula[7], which is the liquid drop mass with pairing correction. The intra-nuclear transition rates are calculated using Pauli-corrected nucleon-nucleon scattering cross-sections[7]. In the thesis adjustment of the mean free path intra-nuclear transitions is made by keeping the mean free path multiplier constant equal to 4 which is the best fit used parameter.

For the pre-equilibrium emission, the particles in the initial configuration n_0 can be neutron, proton or alpha particle. These excitons interact independently with particles below the Fermi level creating either new particle-hole configurations in the

second stage or getting emitted into the continuum. In the thesis $n_0 = 4$ is used, which is equivalent to a break up of the incoming alpha particle in the nuclear potential field above a completely filled Fermi level.

The experimental cross-sections are obtained from EXFOR data source, IAEA [5]. The theoretical and experimental cross-sections are plotted against the projectile energy and are shown in Fig. (3.5)-(3.12). The excitation functions for the theoretical calculations are shown by a solid line (green) for the pre-equilibrium model and with a dash line circular point on it (red line) while the experimental results are shown by a broken line square point on it (yellow line). The cross-sections are measured in *mili – barn* (mb) and the projectile energy in MeV . The experimental data for the reaction channels $^{69}Ga(\alpha, n)^{72}As$ and $^{69}Ga(\alpha, 2n)^{71}As$ is taken from the author V.N. Levkovskij [13]. The data is chosen from the author, because it has the smallest possible errors in both the cross-section and energy measurement. In addition to this the energy points are of lowest size which fits the theoretically used energy size. It can be seen from Fig.(3.5) and (3.6) that the excitation functions both the pre-equilibrium and pure equilibrium models show a Maxwellian curve at low energies by which the reaction mechanism can be explained by the compound nucleus theory. From the figures, it is evident that the pre-equilibrium modified GDH model better agrees with the experimental data than the pure equilibrium model.

The $^{69}Ga(\alpha, 3n)^{70}As$, $^{69}Ga(\alpha, p3n)^{69}Ge$ and $^{71}Ga(\alpha, n)^{74}As$ reaction channels experimental data is taken from authors I.A.Rizvi, M.K. Bhardwaj, M.A Fzal Ansari and A.K Chaubey [14]. It may be seen from Fig.(3.7) that the pre-equilibrium contributions to the excitation function is more significant than the excitation functions in Fig.(3.5) and (3.6). From Fig (3.8) and (3.10), we see that the pre-equilibrium

model is still fits the experimental result but the two curves do not have nearly the same peaks as those in the other figures. In these reaction channels the experimental excitation function peaks more than the theoretically calculated one. This may be explained by considering the fact that at higher energies, the angular momentum imparted by the projectile creates more yrast states which inhibits particle emission. The reactions with proton emission is affected with the Coulomb potential. The effect of this is observed in the shape of the excitation function which shows a barely visible compound nucleus to that of the increasing shape as seen in the Fig. (3.8) of the reaction channel $^{69}\text{Ga}(\alpha, p3n)^{69}\text{Ge}$. In this reaction both the experimental and the theoretical curves show only rising parts showing compound nucleus contributions which is almost insignificant at energies lower than about 40Mev. But it may be seen from this figure that above this energy, the compound nucleus bump is just evident in both theoretical and experimental results. The agreement between the experimental and the theoretical excitation functions can be judged from their peak positions and widths.

As the initial exciton number has an effect in the excitation function of the pre-equilibrium stages of the nuclear reaction, exciton number $n_0 = 4$ and $n_0 = 5$ are taken for the comparison in the reaction channel $^{71}(\alpha, n)^{74}\text{As}$. The theoretical and the experimental excitation functions for these exciton numbers are shown in Fig.(3.11). It can be seen from the figure that for the pre-equilibrium stage the exciton number $n_0 = 4$ and $n_0 = 5$ both fits the experimental curve even though the value $n_0 = 5$ is used throughout the thesis. Another comparison is done to see the effect of the level density on the excitation function. The level density value 9 which is taken for all calculations in the thesis is compared with level density value 10 for the reaction

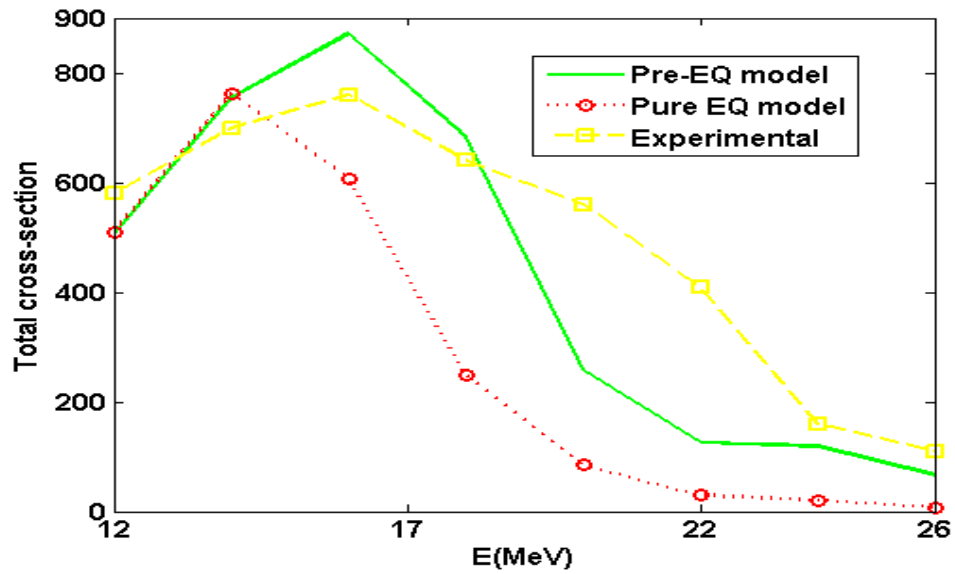


Figure 3.5: Experimental and theoretical excitation function for the reaction ${}^{69}\text{Ga}(\alpha, n){}^{72}\text{As}$

channel ${}^{69}(\alpha, n){}^{72}\text{As}$. The theoretical cross-sections for the two level density values and the experimental cross-sections are shown in Fig.(3.12).The figure show that the value for the level density 9 better fits the experimental curve in the pre-equilibrium region than the level density value 10. It should be noted that all the plots for the cross-sections are measured in *mili – barn(mb)*.

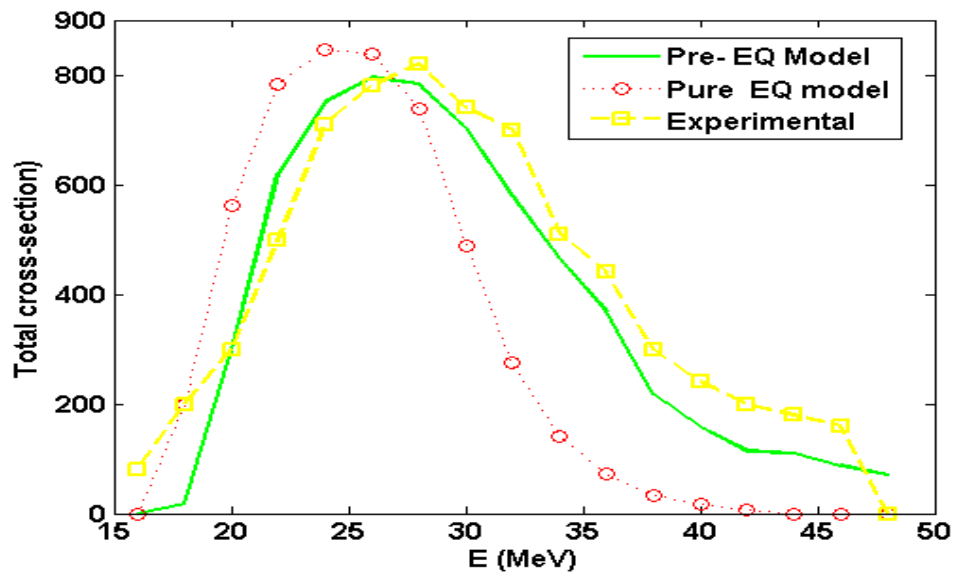


Figure 3.6: Experimental and theoretical excitation function for the reaction $^{69}\text{Ga}(\alpha, 2n)^{71}\text{As}$

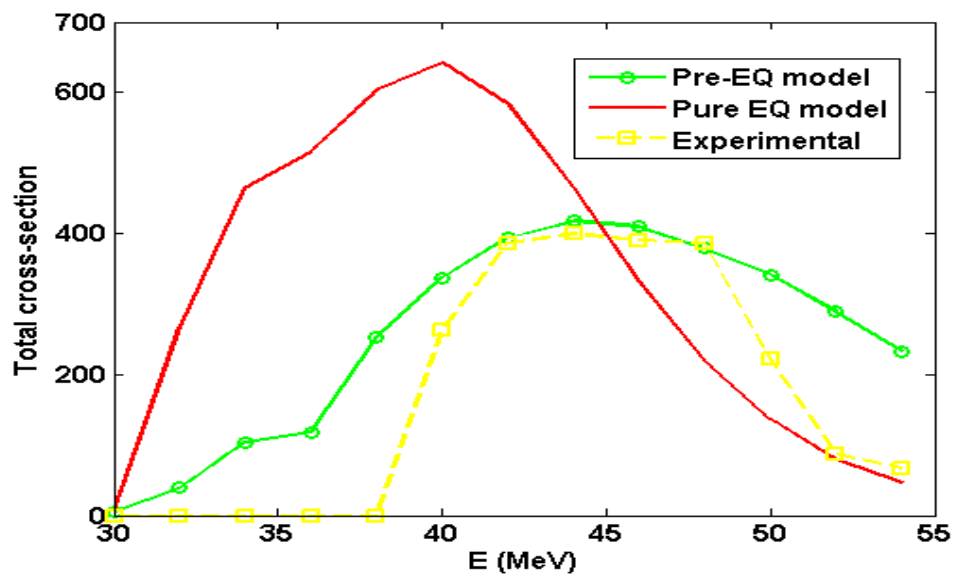


Figure 3.7: Experimental and theoretical excitation function for the reaction $^{69}\text{Ga}(\alpha, 3n)^{70}\text{As}$

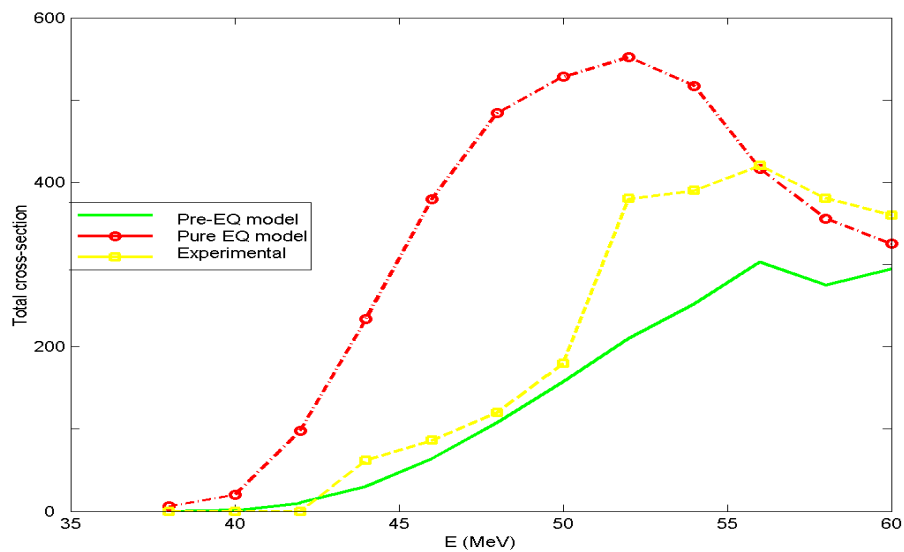


Figure 3.8: Experimental and theoretical excitation function for the reaction ${}^{69}\text{Ga}(\alpha, p3n){}^{69}\text{Ge}$

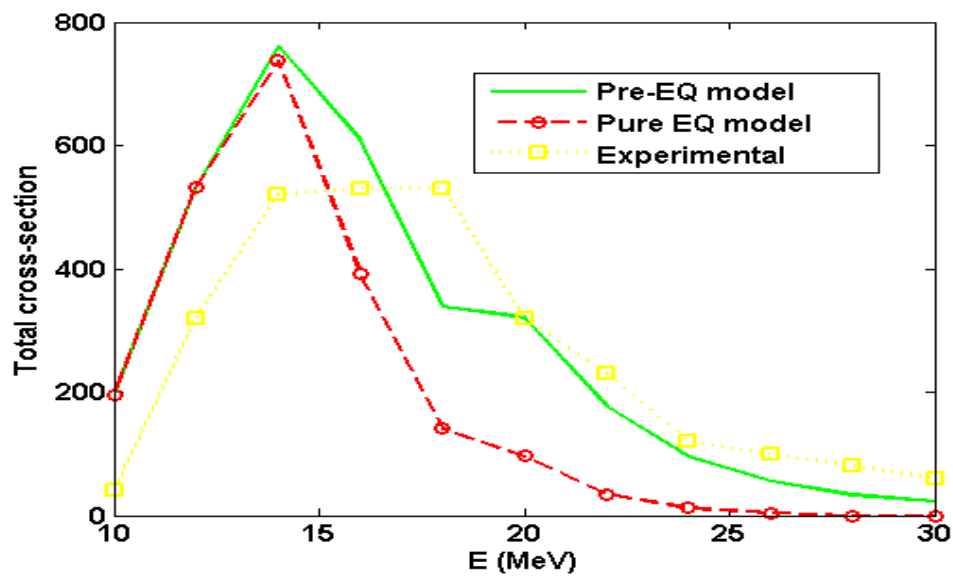


Figure 3.9: Experimental and theoretical excitation function for the reaction ${}^{71}\text{Ga}(\alpha, n){}^{74}\text{As}$

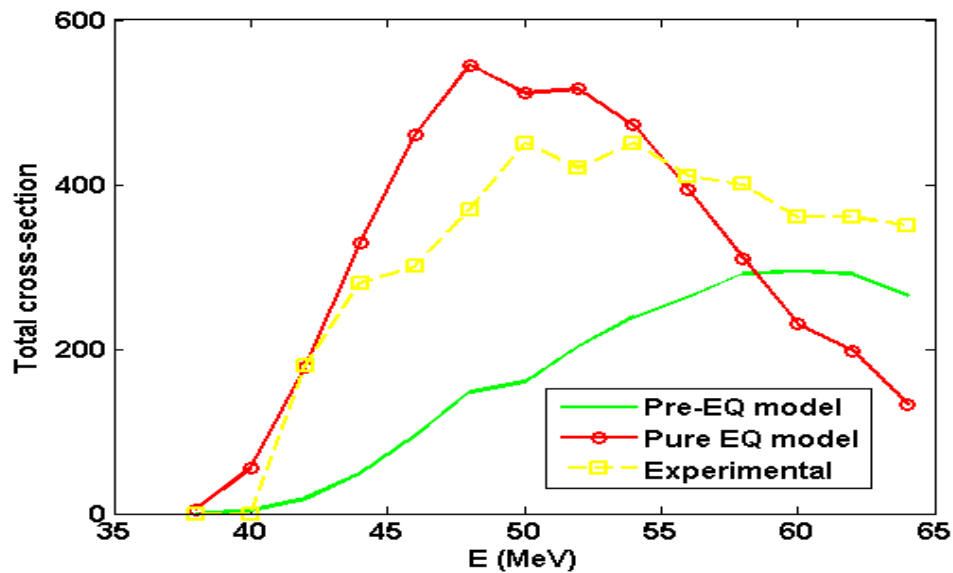


Figure 3.10: Experimental and theoretical excitation function for the reaction $^{71}\text{Ga}(\alpha, 4n)^{71}\text{As}$

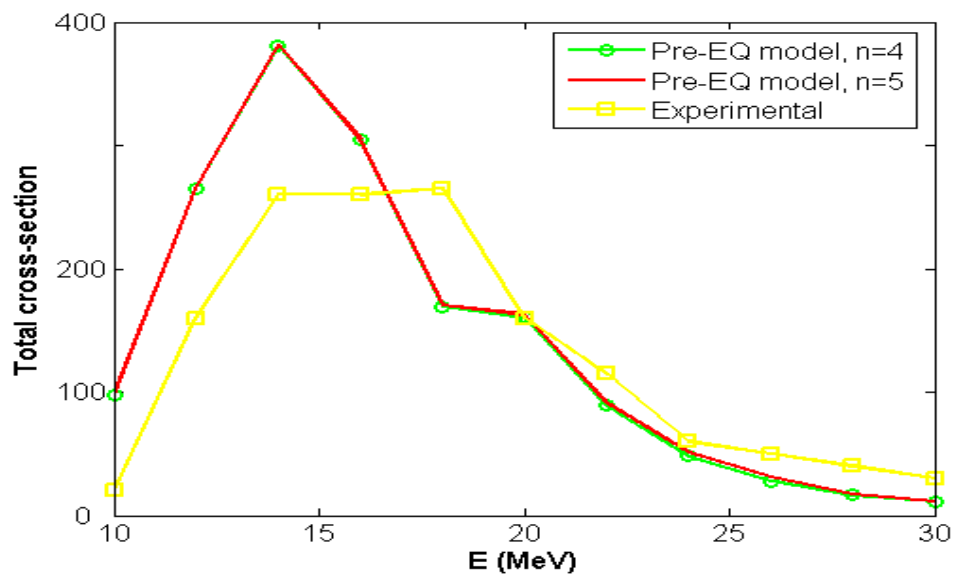


Figure 3.11: Experimental and theoretical excitation function for the reaction $^{71}\text{Ga}(\alpha, n)^{74}\text{As}$ for two exciton numbers.

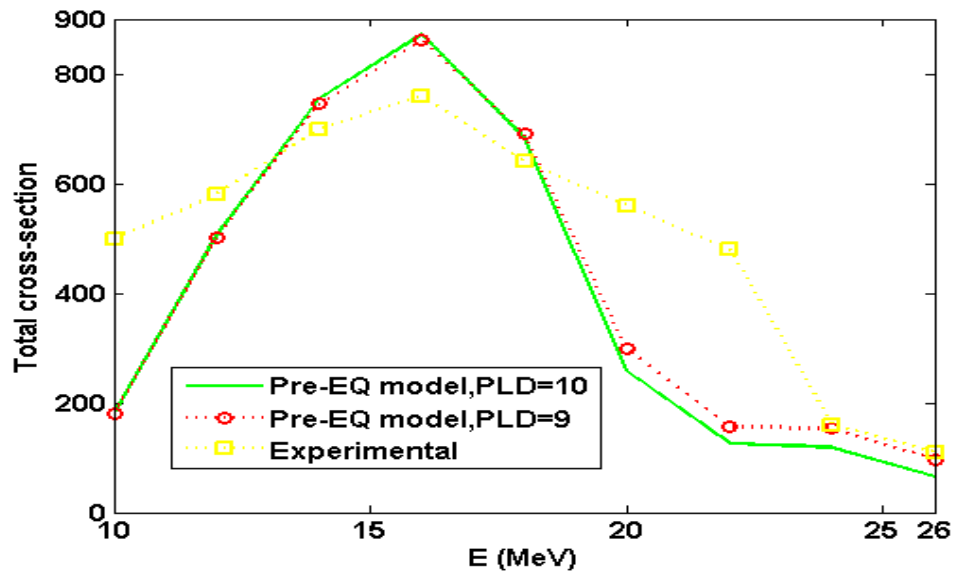


Figure 3.12: Experimental and theoretical excitation function for the reaction $^{69}\text{Ga}(\alpha, n)^{72}\text{As}$ for two level density values

Chapter 4

Summary and Conclusion

4.1 Summary

Nuclear reactions with intermediate projectile energies occurs at two stages. These two stages are the pre-compound and the compound(equilibrium) nucleus stages. For the study of nuclear reactions ,different classical and semi-classical models have been developed. Among the many semi-classical models the geometry dependent hybrid(GDH) model developed by M.Blann reproduces the experimental data in good agreement[3]. The GDH model is the modification of the cascade and exciton model by considering the effect of impact parameter on the reactions.

In the compound nucleus reactions,the projectile is captured by the target nucleus and its energy is shared and re-shared among the nucleons of the target until it reaches a state of statistical equilibrium. After a time much longer than the nuclear transit time, a nucleon or a group of nucleons near the surface receive enough energy to escape just as a molecule evaporates from the heated liquid drop. The statistical process favor the evaporation of nucleons with energy as small as possible above the

threshold energy. The evaporation of nucleons gives a Maxwellian distribution, which is observed from the figures especially at low energies.

In the thesis, for the study of alpha induced reaction on gallium isotopes, the reaction is studied using both the Weisskopf-Ewing model and the pre-equilibrium model of particles using the geometry dependent hybrid model with an improved computer code COMPLETE. The code complete includes maximum angular momentum contributions of the partial wave ($l=0$ to $l=99$). Using the code complete the theoretical excitation functions are computed by supplying standard input parameters of the problem and also the adjustable free parameters for both the compound and pre-equilibrium calculations. The experimental excitation functions are obtained from the EXFOR data source, IAEA. The theoretical and experimental excitation functions for the reaction channels $^{69}\text{Ga}(\alpha, n)^{72}\text{As}$, $^{69}\text{Ga}(\alpha, 2n)^{71}\text{As}$, $^{69}\text{Ga}(\alpha, 3n)^{70}\text{As}$, $^{69}\text{Ga}(\alpha, p3n)^{69}\text{Ge}$, $^{71}\text{Ga}(\alpha, n)^{74}\text{As}$ and $^{71}\text{Ga}(\alpha, 4n)^{71}\text{As}$ are plotted together. The results of the theoretical excitation functions for the pre-equilibrium model generally, can be seen to agree with the experimental results showing that alpha induced nuclear reactions at intermediate energies (10 MeV-70 MeV) occurs through the pre-equilibrium and the compound (equilibrium) stages.

4.2 Conclusion

The conclusion as to how well the results of the models agree with the experimental results is somewhat subjective. We feel that the excitation functions of alpha induced reactions on the two isotopes of gallium ^{69}Ga and ^{71}Ga analyzed using the computer code COMPLETE agree well with the experimental excitation functions. The excitation function of reaction channel which emits proton from the compound nucleus is

influenced by the Coulomb field of the residual nucleus on the emitted nucleus. This effect is observed with barely compound nucleus bump. Finally conclusion may be drawn that nuclear reactions in the intermediate energy region occurs through the pre-equilibrium and compound nucleus stages. This is confirmed by the thesis.

The future trend studying nuclear reaction mechanism, as alpha induced and heavy ion reactions, is to give a full quantum-mechanical description and a better model for the description. Till today many complicated theories have been developed to give quantum mechanical explanation for nucleon-induced reactions. Among these theories the Feshbach, Kerman and Konin [7] is the one which reproduce the observed experimental data better than the semi-classical models applied to explain nuclear reactions.

Bibliography

- [1] M.K Bhardwaj,I.A Rizvi,A.K Chaubey, Phys.Rev.C.Vol 45 No5,2338(1992)
- [2] J.J Griffin,Phys.Rev.Letts.17,478(1966)
- [3] M.Blann,Phys.Rev.Letts.28,757(1972)
- [4] G.D.Harp and J.M.Miller,Phys.Rev.C3,1847(1971)
- [5] EXFOR data source IAEA,Vienna(2004)
- [6] S.N.Goshoshal Atomic and nuclear Physics Vol-3,S.ChandCompany.New Delhi(1997)
- [7] P.E Hodgson Introductory nuclear physics (Clarendon Oxford,1971)
- [8] J.M Blatt and V.F.Weisskopf,Theoretical nuclear physics (Wiley,New York,1952)
- [9] J.Ernest,W.Friedland H.Stockhrest,Z.phys,A-Atomic nuclei 328,333(1987)
- [10] PE Hodgson,Nuclear reactions and nuclear structure(Clarendon,Oxford,1971)
- [11] J.Ernest,Procd.8thInt.conf.onnuclear reaction mechanism(Vienna)June9-14 edited by E.Gadoli(1997)
- [12] A.Calboreanu,Rom.Joourn,vol.51,Nos 9-10,Bucharest(2006)
- [13] V.N Levkovskij,Activation cross-section nuclide of average masses (A=40-100) by protons and alpha particles with average energy(E=10-50Mev),EXFOR data source IAEA(2004).
- [14]I.A Rizvi,M.K Bhardwaj,M.A Fazal,A.K Chaubey et al,Non-equilibrium effects in alpha particle induced reactions on gallium isotopes,EXFOR,data source.
- [15] M.Ismail,Measurement and analysis of excitation functions for alpha induced reactions on gallium and tin isotopes,EXFOR data source IAEA(2004)